MICRO-MECHANISTIC ANALYSIS OF *IN SITU* CRACK GROWTH IN TOUGHENED CARBON/EPOXY LAMINATES TO DEVELOP MICRO-MECHANICAL FRACTURE MODELS

G. Borstnar[a*], M.N. Mavrogordato[a], I. Sinclair[a], S.M. Spearing[a]

[a]*Engineering Materials, University of Southampton, Southampton, United Kingdom*
**G.Borstnar@soton.ac.uk*

Keywords: CFRP, Synchrotron Radiation Computed Tomography, Synchrotron Radiation Computed Laminography, Interlaminar Failure

Abstract
Mode I and Mode II crack growth through particle-toughened CFRPs (Carbon Fibre Reinforced Plastics) have been captured using in situ *and* ex situ *Synchrotron Radiation Computed Tomography (SRCT) and Synchrotron Radiation Computed Laminography (SRCL). These experiments were used to provide non-destructive identification of fracture mechanisms at representative stress states for two different material geometries. The local micro-structure prior to crack propagation, the location of particle/matrix de-bonding events, the formation of bridging ligaments, and the evolution of the resultant crack path was identified and related to the local micro-structure. Such data is invaluable to the development and validation of physically representative micro-mechanical models for these material systems that are increasingly being used in primary aerospace structures.*

1. Introduction

The high specific stiffness and strength of CFRPs makes them desirable for use in aerospace applications, where a reduction in weight directly influences the aircraft's payload and range. However, composites are poor at resisting low velocity impact damage, which will inevitably occur whilst in service. Such events can significantly reduce the residual mechanical properties and are particularly dangerous since damage, in the form of internal delaminations, is difficult to identify from surface inspections and may reduce compressive properties by up to 60% [1]. Attempts to compensate for these issues inevitably leads to over-engineered structures. Given that Mode I and Mode II dominated loading conditions have been identified to occur under low velocity impacts [2], modelling such Mode I and II interlaminar fracture is a key step in developing models for impact damage resistance and post-impact damage tolerance.

An effective way of increasing the toughness of polymer matrices is through the incorporation of secondary phase particles into base matrix [3-5]. The incorporation of such matrices between the plies of a composite, called interlayering, has been shown to increase the interlaminar toughness by several authors [6-9]. While the introduction of interlayers of toughened matrix materials generally increases the delamination resistance, it has been established that an improvement in bulk resin properties does not directly translate to a equal

improvement in toughness, which is often ascribed to the action from the neighbouring, relatively stiff, fibre-reinforced plies [6,7]. Interlayer toughening mechanisms have generally been investigated with post-mortem analysis that cannot directly identify the sequence of damage evolution [6,7].

In this work, crack growth was achieved and observed both *in situ* and *ex situ,* in regions away from free-edges and without the risk of introducing free-surface artefacts. This was achieved in both standard and non-standard specimen geometries with Synchrotron Radiation Computed Tomography (SRCT) and Synchrotron Radiation Computed Laminography (SRCL), techniques that have been used previously to identify damage within CFRPs [10-13]. *In situ* experiments were performed, both under Mode I and Mode II, with samples held at load during the scan. Further Mode II experiments were conducted *ex situ*, in the form of an unloaded three-point bend. This permitted the chronological sequence of local damage evolution to be identified, emphasizing the influence of local microstructural irregularity on the location and geometry of damage initiation and growth. Understanding these processes is key to the development of physically representative micro-mechanical models.

2. Methodology

2.1. Materials

CFRP test coupons were manufactured using a 16-ply (3mm thick) uni-directional lay-up. Intermediate modulus fibres (~5µm in diameter) were used in the proprietary pre-pregs, with a ~30µm particle-toughened interlayer consisting of ~10µm thermoplastic particles. For the Mode I and Mode II specimens seen in Figure 1(a), a 40µm thick PTFE starting defect was inserted into the mid-plane interlayer. To minimize scanning artifacts in SRCT, Geo. 1 specimens were used since the 3x1mm cross-section provided relatively uniform X-ray path lengths at all angles of rotation. Geo. 2 specimens were of a standard geometry in accordance to the British Standard BS ISO 15024:2001 [14].

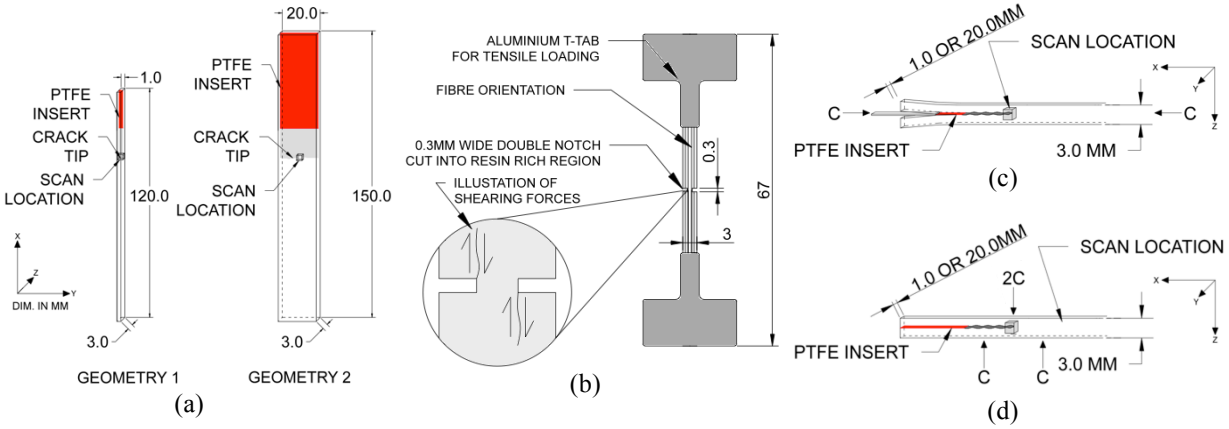

Figure 1. Schematics showing; (a) the narrow and standard specimen geometries, (b) the Mode II *in situ* double-notched specimen geometry, (c) the Mode I *in situ* wedge-loaded configuration and (c) the *ex situ* Mode II loading configuration (where 'C' denotes a compressive force)

2.2. Mode II in *situ double-notched tensile testing*

The double-notched specimen shown in Fig. 1(b) was 67mm long, 3mm thick and 1mm wide. Notches were cut into the resin rich regions to facilitate a Mode II-dominated *in situ* loading

on the resultant cracks. The specimen was loaded in tension using a tensile loading rig compatible to SRCT requirements as described in [12].

2.3. Mode I in situ *testing*

A wedge-loaded double cantilever arrangement was used to provide Mode I loading, in which a wedge was driven into the resin rich region at mid-plane (Fig. 1(c)). Guides ensured correct alignment of the wedge for the Geo. 1 samples, and crack growth was successfully captured in both specimen geometries. Mode II pre-cracks were used to ensure the crack initiated within the resin rich region before the wedge was inserted. This was followed by 1cm of Mode I crack growth to minimize the effects of the Mode II pre-cracking.

2.4. Mode II ex situ *testing*

Mode II cracks were also produced *ex situ* using a three-point bend as shown in Fig. 1(d). Geo. 1 specimens were scanned using SRCT 'post-growth' to provide a more detailed view of the Mode II fracture micro-mechanisms, whilst crack growth was successfully captured using SRCL in Geo. 2 specimens.

2.5. Synchrotron Radiation Computed Tomography and Laminography

SRCT scans were conducted on the I13 beamline at the Diamond Light Source (DLS) in Oxford, UK. A voxel resolution of 1.1μm with a detector size of 2016x2016 pixels was used, and a ~50mm propagation distance was used to take advantage of the phase effect [15]. Scans were also conducted at the Swiss Light Source (SLS) on the TOMCAT beamline in Villigen, Switzerland. A voxel resolution of 0.69μm was achieved with a detector size of 2560x2160 pixels and a propagation distance of ~22mm. Reconstructions were conducted using in-house software at both beamlines.

2.6. Synchrotron Radiation Computed Laminography

SRCL scans were conducted at the European Synchrotron Radiation Facility (ESRF) on the ID19 beamline in Grenoble, France. A voxel resolution of 1.4μm was used with a detector size of 2040x2040 pixels. In SRCL, the sample is rotated about an axis that is at an angle to the plane normal to the specimen. This permits scanning of laterally extended geometries such as Geo. 2, without risking full-attenuation of the beam [16]. The reconstructions were completed using a reconstruction code authored by L. Helfen, with an in-built ring correction to minimise such artefacts in the reconstructed volumes. A comparison of using SRCT and SRCL with regard to identifying damage in CFRPs is described by Bull *et al.* in [10].

3. Results

3.1. Double-notched in situ *load*

Fig. 2 shows a large number bridging ligaments under *in situ* Mode II-dominated loading conditions as illustrated in Fig. 1(b). Fig. 2 shows the wake of the crack, about 1mm behind the first instances of particle de-bonding events. Fig. 2(i) identifies a particularly tortuous region in this CT 'slice', in which the shearing direction can be easily identified by fitting the top and bottom crack surfaces together. The formation of the echelon cracks is complex, and at (ii) we can see that resin from between two particles has been pulled out and torn, in

essence forming a small-scale bridging ligament within the echelon formation. Such behaviour may be promoted by secondary de-bonding events, such as at (iii), that do not coalesce to form the main crack. Substantial cracking along the ply interface can be seen at (iv), in which the crack path is avoiding the particle-depleted region below, indicating that the crack will propagate via a different mechanism when crack coalescence is not possible. Consideration of the geometry of the feature at (v), suggests that this was a particle-bridge, after which the bottom surface of the particle completely de-bonded and was pulled out of its original location. Fig. 2 clearly illustrates the complexity of the fracture in particle-toughened interlayers, in which there is evidence of; macro-scale ligaments featuring micro-scale bridges, secondary de-bonding, and crack path preferentiality.

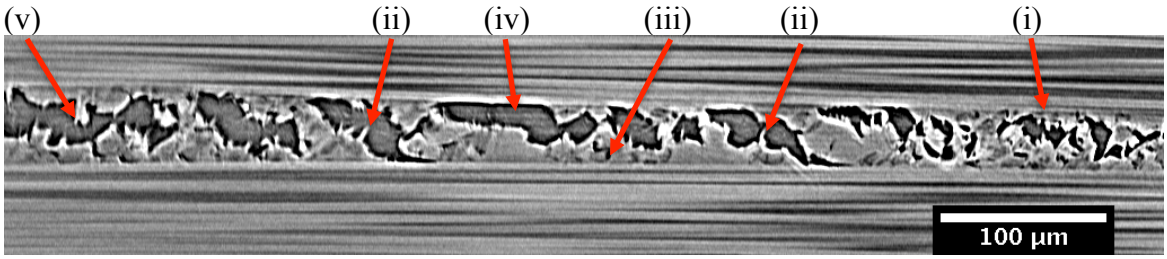

Figure 2. Bridging ligaments under *in situ* Mode II-dominated loading conditions captured at the SLS using SRCT showing; (i) tortuous crack path, (ii) small scale bridging locations, (iii) secondary de-bonding, (iv) ply interface failure, and (v) suspected particle pullout.

3.2. Mode I in situ *growth*

Fig. 3 captures crack growth through a pre-characterised interlayered region in a CFRP, where the top image shows a pre-growth single 'slice' and the bottom image shows the same 'slice' post-growth. At both crack tips, we see evidence of initial particle-de-bonding, with some evidence of bifurcation of the crack at (i). The key differences from Mode II *in situ* cracks, which featured discontinuous echelon arrangements more than 1mm behind the 'tip', is that significant coalescence occurs within 500µm of the initial de-bonding events and that there are substantially fewer bridging ligaments present. Particle-depleted regions at (ii), with particles sparsely located along the top of the interlayer, are shown to have an effect on the resultant crack path (iii), providing evidence that cracks preferentially follow particle-rich regions. In this particular material system, the 3D volume analysed showed that when cracks did not propagate through the coalescence of de-bonded regions, they were more likely to propagate along the ply interface, with events of cracking through neat resin (particle-depleted regions) facilitating the transition to the interface. This suggests that there is a competition between these modes of fracture in which, when one mode is unavailable, the crack will propagate along the next lowest energy path. At (iv), we are able to discern clearly that these loading conditions were Mode I from the crack surfaces separating vertically with no shear present. At (v), a bridging ligament has been captured pre- and post-growth, having broken as the crack propagated, reflecting the principle behaviour captured by cohesive zone models. It is evident that the large bridging ligaments are not present far behind the crack tip in Mode I when compared to Mode II (Fig. 2), and that the density and size of such ligaments should be considered in developing representative models.

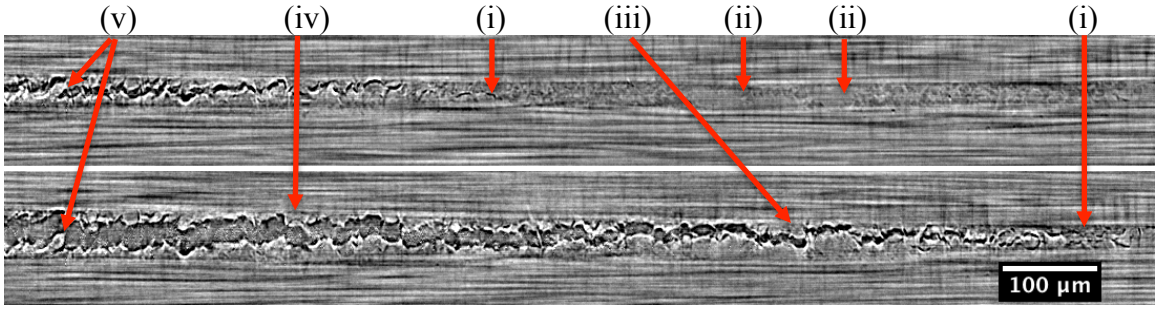

Figure 3. *In situ* Mode I crack growth captured in Geo. 1 specimens using SRCT at DLS showing; (i) a region of bifurcating cracks, (ii) particle depleted regions, (iii) crack path preferentiality, (iv) loading direction (opening, no shear), and (v) a bridging ligament being torn.

Fig. 4 shows an SRCL scan of Mode I crack growth within the standard Geo. 2 specimens. The results show that the relative distance from the initial particle resin de-bonding events to significant coalescence is much faster than in Mode II, supporting observations from the Geo. 1 specimens. However, the white phase fringes forming around the crack faces make the crack surfaces and bridging ligaments more difficult to identify. This is complicated further in that SRCL fills larger spaces between the crack surfaces with a grey-scale value greater than 'zero', evident on the left hand side of the bottom 'slice'. However, the data does importantly validate the micro-mechanisms observed between the specimen geometries in this CFRP system, giving confidence that the behavior of the narrower geometries is representative. Away from large cracks, the microstructure of the material can be identified and there appear to be a few particle/resin de-bonds prior to any loading. This is observed between two large particles at (i), and at some other locations in the interlayer (ii). This shows that the residual stresses in the interlayer, probably caused by processing-induced stresses, are high enough to de-bond the particles, and this may have implications in quality control situations. Microstructural irregularity, as pointed out previously, is also present at (iii) where a substantially large region is particle depleted, and distributions in particle sizes have also been observed.

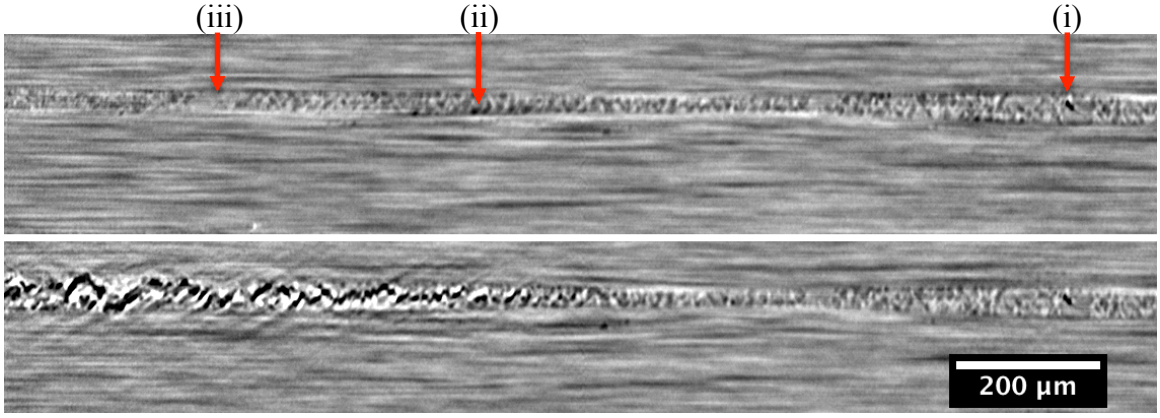

Figure 4. *In situ* Mode I crack growth captured in standard-sized specimens using SRCL at ESRF showing; (i) de-bonding around two large particles prior to loading, (ii) additional pre-existing de-bond locations, and (iii) particle-depleted regions.

3.3. Mode II ex situ *growth*

Fig. 5 shows Mode II crack growth in a standard Geo. 2 specimen. The discontinuous nature of the crack echoes the discontinuous echelons seen in Fig. 2, but due to the lower resolution and phase fringes, the results are of insufficient quality for detailed quantitative analysis when

compared to SRCT. There are some dark spots at location (i), with grey-scale values that are inconsistent with particles, suggesting that there may be some voids present in this region. There also appear to be a few (ii) de-bonding events sparsely located within the interlayer, again suggesting that the residual stress state within the interlayer should be considered in models. Since these samples were unloaded when scanned, whether there were echelon ligaments between the crack faces is unclear. Additionally, the crack captured here is closer to the crack tip than that imaged in Fig. 2, but it is evident that such discontinuous coalescence in Mode II appears to be required for the formation of bridging ligaments, which are much sparser in Mode I.

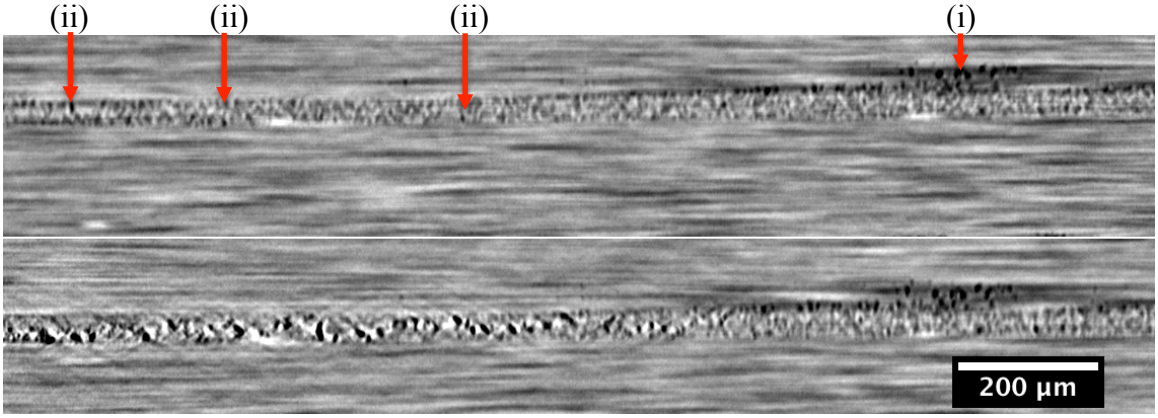

Figure 5. *Ex situ* Mode II crack growth captured in standard-sized specimens using SRCL at ESRF showing a discontinuous crack tip with; (i) suspected voids in the ply, and (ii) de-bonds present prior to loading.

3.3. Quantitative Crack Opening Displacement (COD) analysis

The crack tips of both Mode I *in situ* and Mode II *ex situ* scans were captured in Geo. 1 specimens at the SLS. The higher quality of the 0.69µm scans permitted a COD analysis to be conducted. CODs obtained from SRCT have been used previously by Wright *et al.* to compare and validate notch-tip damage models [12]. In this work, a trainable segmentation plug-in to ImageJ [17] was used, followed by data manipulation in MATLAB [18] to obtain the COD values. This was conducted for a 2D slice in the middle of the scanned volume and the CODs are shown in Fig. 6, where discontinuous cracking was identified whenever the vertical COD (y-axis) was zero. Comparing Fig. 6(a) to (b), we can see that the crack is much more discontinuous in Mode II, with such behaviour extending to at least ~1500pix. (1mm) behind the first segmented crack. The COD also plateau'd between 5-10pix. (~0.7µm). The graph illustrates the problem that has challenged researchers when standardizing the Mode II fracture toughness test, since there is no clear location where the crack tip can be identified. It must be acknowledged that the Mode II crack analysed was unloaded, but *in situ* observations (Fig 2.) support that such discontinuous behaviour continued far behind the tip when under load. Comparing this to Mode I, there appears to be a significant region of coalescence between positions 1200-1400pix, which was only ~0.4mm behind the first identified de-bonds. Additionally, there appears to be a steady increase in COD, which is explained by the *in situ* configuration. The marked differences in Mode I and Mode II reflect the more concentrated stresses on the interlayer at the crack tip in Mode I, when compared to the more global shear displacement of the plies in Mode II.

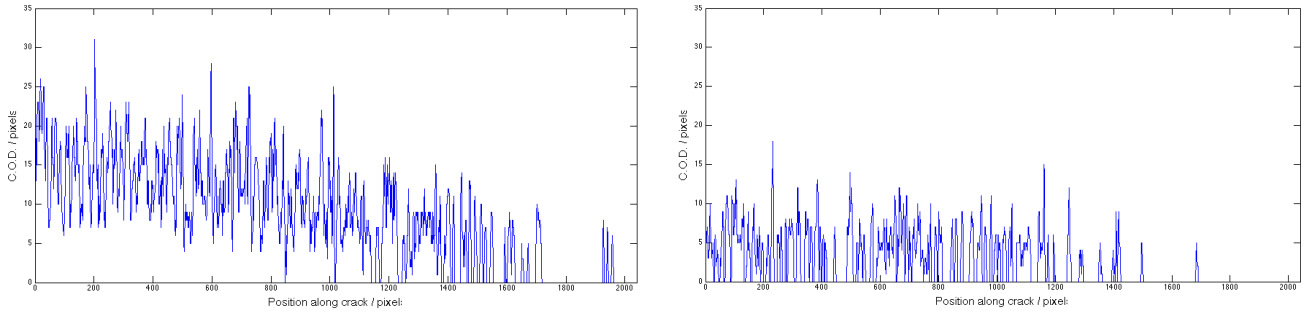

(a) (b)

Figure 6. Plot of COD against position along the crack for (a) Mode I *in situ* and (b) Mode II *ex situ* loading (1pix. = 0.7 um) conducted at the SLS

4. Summary

Overall, experiments have successfully captured Mode I and Mode II crack growth through the complex micro-structures within an interlayer toughened CFRP. The unique use of *in situ* experiments has evidenced bridging ligaments in action, with particular detail visible in the Mode II–dominated condition where larger echelon ligaments featured secondary bridges formed from the resin between particles being pulled out and torn. Such ligamented behaviour lends itself towards the use of cohesive zone models, but the challenge is still to identify the correct traction-separation laws to use from the constituent microstructure and hence, determine which microstructure is required for optimal performance. In all of the data presented, it is clear that the process of delamination propagation is much more of a damage evolution process, in which a single crack forms through crack coalescence of previous damage within the interlayer. The much more discontinuous nature of the Mode II crack, identified via SRCL, and the subsequent existence of more bridging ligaments than in Mode I, suggests that such behaviour is required to promote bridging. It was observed that Mode I cracks coalesced much faster than in Mode II with fewer bridging locations, and the relative speed of coalescence between the two loading conditions was supported by quantitative COD analysis. Evidence of particles de-bonding prior to loading suggests that a significant amount of residual stress is present within the interlayer that should also be accounted for in models.

Acknowledgements

The authors gratefully acknowledge Cytec Engineered Materials for financial and materials support, and the support from staff at the μ-VIS X-Ray Imaging Centre, Southampton University. The authors acknowledge the staff at the TOMCAT/SLS and I13/DLS beamline, and Lukas Helfen and staff at the ID19/ESRF beamline. Finally, the authors acknowledge Tomasz Cwik and Serafina Consuelo Garcea for sharing their valuable SRCL and SRCT time.

References

[1] A. T. Rhead, R. Butler, and N. Baker. Analysis and compression testing of laminates optimised for damage tolerance. *Appl. Comp. Mat.,* vol. 18, pp. 85–100, 2011.

[2] C. Bouvet, S. Rivallant, and J. J. Barrau. Low velocity impact modeling in composite laminates capturing permanent indentation. *Comp. Sci. Tech.*, vol. 72, no. 16, pp. 1977–1988, 2012.

[3] S.-Y. Fu, X.-Q. Feng, B. Lauke, and Y.-W. Mai. Effects of particle size, particle/matrix interface adhesion and particle loading on mechanical properties of particulate–polymer composites. *Comp. Part B* , vol. 39, no. 6, pp. 933–961, 2008.

[4] Garg, A. C. Failure Mechanisms in Toughened Epoxy Resins - A Review. *Comp. Scie. and Tech*., vol. 31, pp. 179–223, 1988.

[5] M. Zamanian, M. Mortezaei, B. Salehnia, and J. E. Jam. Fracture toughness of epoxy polymer modified with nanosilica particles: Particle size effect. *Eng. Fract. Mech.*, vol. 97, pp. 193–206, 2013.

[6] M. R. Groleau, Y. Shi, A. F. Yee, J. L. Bertram, H. J. Sueb, and P. C. Yang. Mode II Fracture of Composites Interlayered with Nylon Particles. *Comp. Sci. Tech.*, vol. 56, pp. 1223–1240, 1996.

[7] S. Singh and I. K. Partridge. Mixed-Mode Fracture in an Interleaved Carbon-Fibre/Epoxy Composite. *Comp. Sci. Tech.*, vol. 55, no. 95, 1996.

[8] M. Hojo, S. Matsuda, M. Tanaka, S. Ochiai, and A. Murakami. Mode I delamination fatigue properties of interlayer-toughened CF/epoxy laminates. *Comp. Sci. Tech.*, vol. 66, no. 5, pp. 665–675, May 2006.

[9] M. Yasaee, I. P. Bond, R. S. Trask, and E. S. Greenhalgh. Mode I interfacial toughening through discontinuous interleaves for damage suppression and control. *Comp. Part A,* vol. 43, no. 1, pp. 198–207, Jan. 2012.

[10] D. J. Bull, L. Helfen, I. Sinclair, S. M. Spearing, and T. Baumbach. A comparison of multi-scale 3D X-ray tomographic inspection techniques for assessing carbon fibre composite impact damage. *Comp. Sci. Tech.*, vol. 75, pp. 55–61, Feb. 2013.

[11] A. E. Scott, M. Mavrogordato, P. Wright, I. Sinclair, and S. M. Spearing. In situ fibre fracture measurement in carbon–epoxy laminates using high resolution computed tomography. *Comp. Sci. Tech.*, vol. 71, no. 12, pp. 1471–1477, Aug. 2011.

[12] P. Wright, A. Moffat, I. Sinclair, and S. M. Spearing. High resolution tomographic imaging and modelling of notch tip damage in a laminated composite. *Comp. Sci. Tech.*, vol. 70, no. 10, pp. 1444–1452, Sep. 2010.

[13] A. J. Moffat, P. Wright, L. Helfen, T. Baumbach, G. Johnson, S. M. Spearing, and I. Sinclair. In situ synchrotron computed laminography of damage in carbon fibre–epoxy [90/0]s laminates. *Scr. Mater.*, vol. 62, no. 2, pp. 97–100, Jan. 2010.

[14] Fibre-Reinforced Plastic Composites - Determination of Mode I interlaminar fracture toughness, GIC, for unidirectionally reinforced materials, Tech. Rep. BS ISO 15024:2001, *British Standard* BSi, 2001.

[15] P. Cloetens, M. Pateyron-Salomé, J. Y. Buffière, G. Peix, J. Baruchel, F. Peyrin, and M. Schlenker. Observation of microstructure and damage in materials by phase sensitive radiography and tomography. *J. Appl. Phys.*, vol. 81, no. 9, p. 5878, 1997.

[16] L. Helfen, A. Myagotin, A. Rack, P. Pernot, P. Mikulík, M. Di Michiel, and T. Baumbach. Synchrotron-radiation computed laminography for high-resolution three-dimensional imaging of flat devices. *Phys. Status Solidi*, vol. 204, no. 8, pp. 2760–2765, Aug. 2007.

[17] W. S. Rasband, "ImageJ." *National Institute of Health*, http://imagej.nih.gov/ij/, Bethesda, Maryland, USA, 2012.

[18] MATLAB and Statistics Toolbox Release 2012b, *The MathWorks, Inc.*, Natick, Massachusetts, United States.